Journal of
Mechanics of
Materials and Structures

A MODEL FOR THE SHEAR DISPLACEMENT DISTRIBUTION OF A FLOW LINE IN THE ADIABATIC SHEAR BAND BASED ON GRADIENT-DEPENDENT PLASTICITY

Xue-Bin Wang and Bing Ma

Volume 7, No. 8-9 October 2012

msp

JOURNAL OF MECHANICS OF MATERIALS AND STRUCTURES
Vol. 7, No. 8-9, 2012
dx.doi.org/10.2140/jomms.2012.7.735

A MODEL FOR THE SHEAR DISPLACEMENT DISTRIBUTION OF A FLOW LINE IN THE ADIABATIC SHEAR BAND BASED ON GRADIENT-DEPENDENT PLASTICITY

XUE-BIN WANG AND BING MA

Based on second-order gradient-dependent plasticity (GDP), we establish the shear displacement distribution of material points of a flow line beyond the occurrence of the adiabatic shear band (ASB) at a position on a thin-walled tubular specimen in dynamic torsion. In the ASB, the shear displacements of a material point include two parts caused by homogeneous and inhomogeneous strain components, respectively. The former is assumed to be a linear function of the material point coordinate, while the latter is found to be a sinusoidal function of the coordinate due to the microstructural effect. For the Ti-6Al-4V alloy and two kinds of steels, the coefficients of the constant, linear, and nonlinear terms in the expression for the shear displacement distribution are determined by least-squares fitting for different widths and positions of the ASB. During the localized shear process, the coefficients of the linear and nonlinear terms are found to have increasing tendencies, while the deformed ASB width (which is larger than the width of the ASB central region) is slightly decreased. This investigation shows that second-order GDP may be successfully applied in simulation of the shear displacement distribution of material points at flow lines in the ASBs.

1. Introduction

Thin-walled tubular metal specimens, providing a homogeneous state of stress [Bai and Bodd 1992], are usually subjected to adiabatic shear failures in dynamic torsional experiments. Dynamic experiments can create a high enough strain rate in the tested materials that the condition for the occurrence of adiabatic shear bands (ASBs) is satisfied, that is, thermal softening outweighs plastic hardening. To observe the initiation and development of ASBs, many fine grid lines are deposited photographically on the outside surface of a specimen before experiments [Giovanola 1988; Marchand and Duffy 1988; Duffy and Chi 1992; Cho et al. 1993; Liao and Duffy 1998]. Initially, these lines are oriented parallel to the axis of the specimen; see Figure 1(a). During the deformation, high-speed photographs of grid lines are taken, in which the slopes of lines provide a measure of the shear strain distribution along the gage length; see Figure 1(b–d).

Marchand and Duffy [1988] conducted dynamic torsional experiments on steels, and concluded that the plastic straining process might be divided into three consecutive stages; see Figure 1(b–d). In the first stage, the grid lines incline but remain straight, which implies that shear deformation within the specimen is homogeneous. In the second stage, the grid lines become slightly curved, as in Figure 1(c), indicating inhomogeneous or localized deformation. Curved grid lines are usually called flow lines. In

Keywords: adiabatic shear band, shear displacement distribution, fitting least-squares method, gradient-dependent plasticity, Ti-6Al-4V, steel.

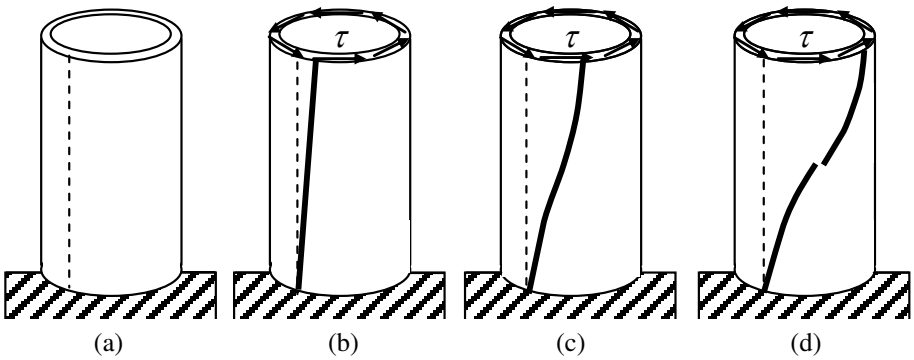

Figure 1. A thin-walled tube specimen without deformation (a), the uniform shear deformation in the elastic and strain-softening stages (b), the nonuniform deformational stage (c), and the discontinuous deformational stage (d). The dotted straight line is the initial grid line parallel to the axis of the specimen. The thick straight and curved lines are the curved flow lines, and τ is the shear stress acting on the sectional area of the specimen.

this stage, shear strain begins to concentrate first in a broad deformed ASB, and then, as deformation continues, becomes more localized until a narrow ASB is formed, marking the beginning of the third stage. In the third stage, flow lines appear discontinuous, as in Figure 1(d), indicating the formation of macroscopic fractures. ASBs are found to begin in the second stage, especially its later stage. Accordingly, the measured shear stress-nominal shear strain curve shows three distinct stages: a sharp rise in stress, followed by a long plateau, and then a steep drop in stress. In general, many kinds of steels and titanium alloys follow this process of deformation [Giovanola 1988; Marchand and Duffy 1988; Duffy and Chi 1992; Cho et al. 1993; Liao and Duffy 1998].

The nonlinear shear displacement distribution of material points at a flow line suggests that different points have different shear strains. Approximately, different material points may possess the same shear stress due to the use of a thin-walled tubular metal specimen. The phenomenon of the same shear stress corresponding to different shear strains cannot be uniquely described by classical continuum models where no internal length parameter is included, so that the nonuniform strain distribution and nonlinear displacement distribution in the localized zone, as well as the zone size, cannot be accurately obtained. Among the enriched continuum models, nonlocal and gradient continua have been widely used to avoid pathological localization in numerical simulation [De Borst and Mühlhaus 1992; Pamin and De Borst 1995; Askes et al. 2000; Menzel and Steinmann 2000; Peerlings et al. 2001; Simone et al. 2004; Voyiadjis and Abu Al-Rub 2005; Peerlings 2007; Poh et al. 2011], as have the Cosserat continuum and viscoplastic theories [Bažant and Pijaudier-Cabot 1988; Shawki and Clifton 1989]. In gradient continua, second-order gradient-dependent plasticity (GDP) is usually adopted, and a few analytical solutions of the strain and strain rate distribution in the localized band have been derived in the one-dimensional tensile and shear cases [De Borst and Mühlhaus 1992; Pamin and De Borst 1995; Menzel and Steinmann 2000]. However, a bilinear (linearly elastic and strain-softening) constitutive relation is used, and no plastic strain occurs within the specimen before strain localization. These assumptions are possibly even applicable for brittle materials, such as rocks, concretes, and ceramics, not just for metal materials, such as titanium alloys

and steels. For these metal materials in dynamic torsion, the measured shear stress-nominal shear strain curve enters a wide plateau stage prior to the localized shear deformation due to shear yield [Giovanola 1988; Marchand and Duffy 1988; Duffy and Chi 1992; Cho et al. 1993; Liao and Duffy 1998].

Assuming that the plastic shear strain corresponding to the ASB onset (also called *critical plastic shear strain*) is not zero, an expression for the local plastic shear strain in the ASB was derived for arbitrary strain-softening materials based on second-order GDP [Wang 2006a; 2006b]. This expression is an even more general formulation than expressions in [De Borst and Mühlhaus 1992; Pamin and De Borst 1995; Menzel and Steinmann 2000], applicable for metal materials. Introducing Johnson–Cook and Zerilli–Armstrong models in the expression, the shear strain, shear displacement, and temperature distribution in the ASB were studied for some metals and alloys in [Wang 2006a; 2006b; 2006c; 2007]. If the local temperature in the deformed ASB exceeds the transformation temperature, then a transformed ASB can appear at the central part of the deformed ASB. The transformed ASB thickness, local plastic shear strain, and shear displacement at interfaces between the deformed and transformed ASBs were investigated [Wang 2008]. The usually reported ASB width is the size of the ASB central region, rather than the total thickness of the deformed ASB. The ASB thickness at the central region was defined as the width of the region surrounding the ASB center over which the temperature differed from its peak value by less than 5% [Wang 2009], and effects of all parameters on the ASB thickness at the central region were studied. The peak and average temperatures in the ASB were calculated from the shear stress-average plastic shear strain curve of the ASB, which was back-calculated from the measured shear stress-nominal shear strain curve of the specimen [Wang 2010].

Based on second-order GDP, the aim of the present study is to discuss the applicability of an expression for the shear displacement distribution of material points at a flow line in dynamic torsion. Based on an expression for the local plastic shear strain in the ASB based on second-order GDP [Wang 2006a; 2006b; 2010], we proposed an expression for the local shear displacement around the ASB considering the following two assumptions: first, the plastic shear strain outside the ASB is treated as uniform, and does not change during the localized shear deformation; second, certain elastic shear strains are stored within the ASB and outside. After establishing the expression, for different widths and positions of the ASB, the experimental data about the shear displacement distribution and evolution with loading time or straining for three kinds of metal materials are fitted using least-squares methods. Among the candidate widths and positions of the ASB, the values minimizing the squared errors are believed to be true. The coefficients of the constant, linear, and sinusoidal terms in the expression are presented, together with their evolution with loading time or straining, and the deformed ASB widths.

2. Shear displacement distribution of a flow line

Before an ASB is initiated, the shear strain within a specimen in torsion can be seen as uniform. After the occurrence of the ASB, the shear strain within the specimen becomes nonuniform. At the ASB position, the local shear strain is higher and increases with straining, while outside the ASB, the local shear strain is relatively lower and approximately remains constant. Figure 2 shows an ideal model for the shear displacement distribution within the gage length after an ASB appears. The model includes three parts: one middle ASB, shown in part (b) of the figure, and two surrounding regions with uniform deformations, shown in parts (a) and (c).

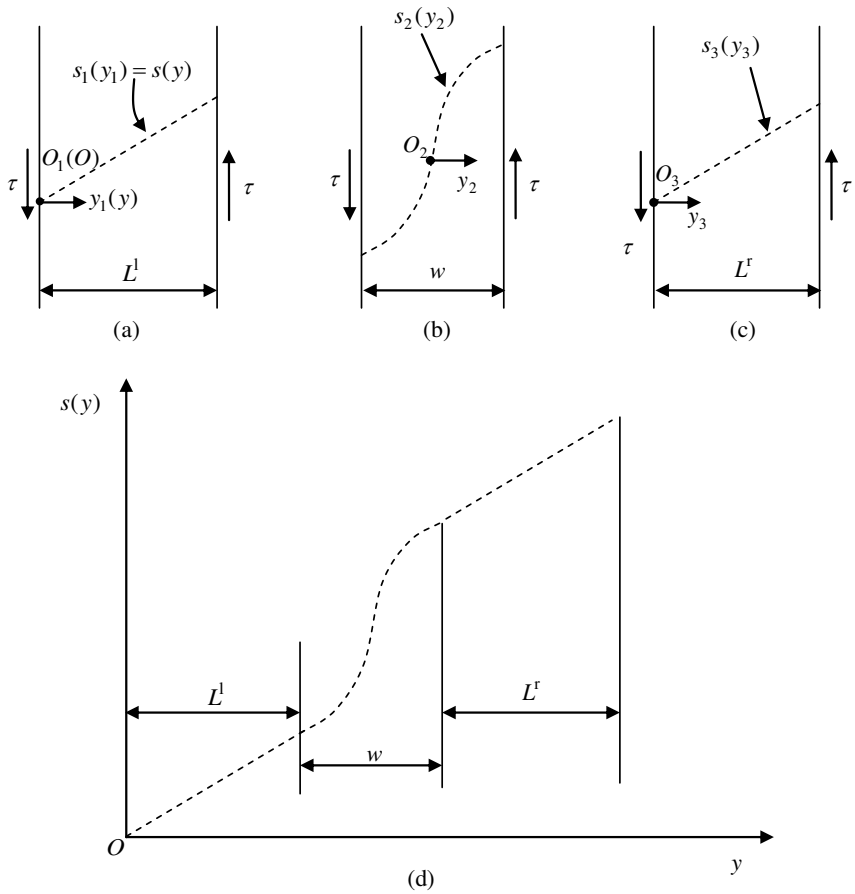

Figure 2. An ideal model for the shear displacement distribution of a flow line within the gage length: (a) the uniformly deformational region at the left side of the ASB, (b) the central deformed ASB, (c) the uniformly deformational region at the right side of the ASB, and (d) the continuous shear displacement distribution of material points at a flow line.

Based on second-order GDP, for a one-dimensional shear problem, an expression for the local plastic shear strain $\gamma_p(y)$ in the ASB was derived [Wang 2006a; 2006b; 2010]:

$$\gamma_p(y_2) = \gamma_c + (\bar{\gamma}_p - \gamma_c)\left(1 + \cos\frac{y_2}{l}\right), \tag{1}$$

where y_2 is the coordinate whose origin O_2 is set at the ASB center (Figure 2(b)); $\bar{\gamma}_p$ (also called the nonlocal plastic shear strain [Menzel and Steinmann 2000]) is the average plastic shear strain of the ASB, which is a variable dependent on the level of shear stress acting on the ASB during the localized shear process; γ_c is the critical plastic shear strain; and l is the internal length parameter in GDP, describing the effect of microstructures of heterogeneous metal materials. The critical plastic shear strain is referred to as the average plastic shear strain corresponding to the onset of the ASB. Prior to the occurrence of the

ASB, certain plastic shear strains have accumulated within metal materials. When the accumulated strain reaches the critical strain, then an ASB takes place. After the occurrence of the ASB, the accumulated strain is increased continuously. In GDP, the spatial gradient terms of plastic strain and their coefficients enter the yield function in order to describe interactions and interplay among microstructures [Askes et al. 2000; Peerlings et al. 2001]. The internal length parameter is believed to be related to the average grain diameter [Peerlings et al. 2001], defining the size of the localized band in numerical and analytical results. Otherwise, pathological numerical results will occur once standard continuum models are used in numerical models. For metal materials, such as Ti-6Al-4V alloy, grains ranged from 2–10 μm in diameter [Liao and Duffy 1998]. During shear deformation, grains can be rotated and elongated along the shear direction, and intense slip lines within grains are well-aligned with the shear direction, as found through transmission electron micrographs [Liao and Duffy 1998]. These observations suggest that interactions and interplay are more intense during the process of localized deformation, and must be taken into account.

Equation (1) is applicable for linear and nonlinear strain-softening cases at postpeak. Moreover, when strain localization is just initiated, the nonzero plastic shear strain accumulated within metal materials due to shear yield is permitted, that is, $\gamma_c > 0$. It is usually assumed that shear stress τ reaches its maximum $\tau_{\max}$ when the ASB just appears via instability analysis. In fact, (1) is also applicable for the case that the ASB appears beyond the peak stress. Rittel et al. [2006] argued that energy factors are the main criterion for the onset of ASB failure, while the strain or stress criterion applies in more restricted conditions.

For a one-dimensional shear problem, an expression for the local shear strain in the localized shear band was derived in [Menzel and Steinmann 2000]. It is only applicable for linear strain-softening materials at postpeak. Equation (1) can be seen as a generalization from this expression. Neglecting the plastic shear strain accumulated within the materials before the localized shear deformation, that is, $\gamma_c = 0$, (1) is simplified as

$$\gamma_p(y_2) = \bar{\gamma}_p\left(1 + \cos\frac{y_2}{l}\right). \tag{2}$$

This means that the localized shear is initiated just at the end of the linear elastic stage. For the linear strain-softening case at postpeak, $\bar{\gamma}_p$ is related to the shear stress difference $\tau_c - \tau$ and the softening modulus c (positive for strain-softening materials):

$$\bar{\gamma}_p = \frac{\tau_c - \tau}{c}. \tag{3}$$

In fact, (2) and (3) are identical to the expression in [Pamin and De Borst 1995]. Differentiating (2) on both sides with respect to time leads to

$$\dot{\gamma}_p(y_2) = -\frac{\dot{\tau}}{c}\left(1 + \cos\frac{y_2}{l}\right). \tag{4}$$

Equation (4) is identical to the result in [Pamin and De Borst 1995]. The derivation of (1) is similar to [De Borst and Mühlhaus 1992; Pamin and De Borst 1995; Menzel and Steinmann 2000]. In these studies, the shear band width w is

$$w = 2\pi l. \tag{5}$$

It is found from (1) that at the ASB's two boundaries ($y_2 = \pm w/2$), $\gamma_p(\pm w/2) = \gamma_c$, while at its center ($y_2 = 0$), $\gamma_p(0) = \gamma_c + 2(\bar{\gamma}_p - \gamma_c)$. At this position, the local plastic shear strain reaches its maximum. Therefore, the plastic shear strain distribution in the ASB is nonuniform. The value of γ_c may be specific for a material if the strain rate and ambient temperature are known. During the localized deformational process, $\bar{\gamma}_p$ ($\bar{\gamma}_p \geq \gamma_c$) is increased with straining. Thus, the profile of the local plastic shear strain becomes steeper until a final fracture occurs.

Herein, differentiating (1) one time with respect to the coordinate y_2 results in

$$\frac{d\gamma_p(y_2)}{dy_2} = -\frac{\bar{\gamma}_p - \gamma_c}{l} \sin\frac{y_2}{l}. \tag{6}$$

Differentiating (6) leads to

$$\frac{d^2\gamma_p(y_2)}{dy_2^2} = -\frac{\bar{\gamma}_p - \gamma_c}{l^2} \cos\frac{y_2}{l}. \tag{7}$$

Thus, using (1) and (7), we have

$$\gamma_p(y_2) + l^2 \frac{d^2\gamma_p(y_2)}{dy_2^2} = \bar{\gamma}_p. \tag{8}$$

In fact, (8) is a special case of (explicit) GDP [Peerlings et al. 2001], that is, one-dimensional GDP in simple shear. Equation (8) establishes a relation between the local $\gamma_p(y_2)$ and nonlocal $\bar{\gamma}_p$ variables. The nonlocal variable is related to the shear stress, which is the plastic shear strain in the context of classical elastoplastic theories. When the nonlocal variable $\bar{\gamma}_p$ and the critical plastic shear strain γ_c are specific, different material points will have different local plastic shear strains, and a unique solution can be ensured. Averaging these local plastic shear strains over the entire ASB will lead to the nonlocal plastic shear strain, as can be easily confirmed through integrating (1) with respect to the coordinate y_2 ($\int_{-w/2}^{w/2} \gamma_p(y_2)\,dy_2$), and then divided by the ASB width. For two and three-dimensional cases, the Laplacian will appear in GDP [Askes et al. 2000; Peerlings et al. 2001; Simone et al. 2004; Voyiadjis and Abu Al-Rub 2005; Peerlings 2007; Poh et al. 2011]. GDP can be derived from the nonlocal theory [Askes et al. 2000; Peerlings et al. 2001] by expanding the plastic strain into a Taylor series, and by neglecting gradient terms of order four and higher.

Integrating (1) with respect to the coordinate y_2, the local plastic shear displacement $s_p(y_2)$ in the ASB can be obtained:

$$s_p(y_2) = \int_0^{y_2} \gamma_p(y_2)\,dy_2 = \bar{\gamma}_p y_2 + l(\bar{\gamma}_p - \gamma_c) \sin\frac{y_2}{l}. \tag{9}$$

Equation (9) describes the relative shear displacements of different material points in the y_2 direction with respect to the origin O_2. Evolution of shear displacements of different material points on the outside surface of a specimen can be measured through high-speed photography of a grid pattern previously printed on the specimen's outer surface [Giovanola 1988; Marchand and Duffy 1988; Duffy and Chi 1992; Cho et al. 1993; Liao and Duffy 1998]. Initially, fine lines are oriented parallel to the axis of the specimen; then, during the deformation, the slopes of lines will change, providing a measure of the local shear strain distribution along the axis of the specimen. Curved flow lines describe the local deformational characteristics within the entire gage section, not only within the ASB; see Figure 2(d).

During the deformational process, certain recoverable elastic shear strains γ^e will be stored within the specimen. These parts of the strains can be seen as uniform. Thus, the total shear displacement $s_2(y_2)$ in the ASB can be expressed as

$$s_2(y_2) = s_p(y_2) + s^e = (\bar{\gamma}_p + \gamma^e)y_2 + l(\bar{\gamma}_p - \gamma_c)\sin\frac{y_2}{l}, \tag{10}$$

where s^e is the elastic shear displacement caused by γ^e.

For the sake of simplicity, the plastic shear strain outside the ASB can be also treated as uniform, equal to γ_c. This suggests that it no longer increases during the localized shear process. Thus, the relative shear displacements with respect to origins O_1 and O_3 in two uniformly deformational regions — see Figure 2(a, c) — can be given by

$$s_1(y_1) = (\gamma_c + \gamma^e)y_1, \tag{11}$$

$$s_3(y_3) = (\gamma_c + \gamma^e)y_3, \tag{12}$$

where $y_1 \in [0, L^l]$, $y_3 \in [0, L^r]$, and L^l and L^r are the sizes of the uniformly deformational regions on the left and right sides of the ASB, respectively. A coordinate transformation is introduced to replace y_2 and y_3 with y_1. Let $y_1 = y$ whose origin O is also set at O_1. Thus, we have

$$y_2 = y - \frac{w}{2} - L^l, \quad y_3 = y - w - L^l. \tag{13}$$

For $y \in [0, L^l]$, the local shear displacement $s(y)$ relative to the origin O according to (11) is

$$s(y) = (\gamma_c + \gamma^e)y. \tag{14}$$

When $y \in [L^l, L^l + w]$, $s(y) = s(L^l) + s_2(y_2) + (\bar{\gamma}_p + \gamma^e)w/2$. Thus, $s(y)$ can be written as

$$s(y) = (\gamma_c + \gamma^e)L^l + (\bar{\gamma}_p + \gamma^e)(y - L^l) + l(\bar{\gamma}_p - \gamma_c)\sin\frac{y - w/2 - L^l}{l}. \tag{15}$$

Apparently, when $y = L^l$, $s(L^l) = (\gamma_c + \gamma^e)L^l$; when $y = L^l + w$, $s(L^l + w) = (\gamma_c + \gamma^e)L^l + (\bar{\gamma}_p + \gamma^e)w$. When $y \in [L^l + w, L^l + L^r + w]$, we have

$$s(y) = (\gamma_c + \gamma^e)L^l + (\bar{\gamma}_p + \gamma^e)w + (\gamma_c + \gamma^e)(y - L^l - w). \tag{16}$$

It can be found from (14)–(16) that at the outside of the ASB, the local shear displacement is a linear function of the coordinate y, and that at the position of the ASB, it is a nonlinear function. The coefficients of the constant, linear, and nonlinear terms are not easy to determine mainly due to the geometrically inhomogeneous deformation defects and inertial effect. Therefore, these coefficients require a fitting.

3. Fitting least-squares method

Four flow lines (#1–#4) in Table 1 are selected for fitting. All tests are conducted under dynamic torsional conditions by use of a torsional split Hopkinson bar [Giovanola 1988; Marchand and Duffy 1988; Cho et al. 1993; Liao and Duffy 1998]. Only high-speed photographs of the grid pattern taken during the formation of the ASB are presented in [Marchand and Duffy 1988; Cho et al. 1993; Liao and Duffy 1998]. However, a time sequence of the shear displacement profiles has been provided [Giovanola 1988]. These profiles are obtained by digitizing a flow line in high-speed photographs, and then smoothing the

Flow lines	Material	Nominal strain rate	Stress or strain state	Flow line data origin
#1	4340 steel	$6000\,s^{-1}$	After strain localization from 45–52.5 μs	[Giovanola 1988, Figure 4]
#2	Ti-6Al-4V	$1100\,s^{-1}$	Before rapid stress drop for frames #1–#4	Frames #1–#5 in [Liao and Duffy 1998, Figure 5]
#3	HY-100 steel	$1200\,s^{-1}$	Prior to the stress peak for frame #4	Frames #4 and #5 in [Cho et al. 1993, Figures 1 and 2]
#4	HY-100 steel	$1600\,s^{-1}$	After the stress peak	Frames "camera #2" and "camera #3" in [Marchand and Duffy 1988, Figure 14]

Table 1. Selected four flow lines from dynamic torsional tests.

digitized records. In order to obtain the relative shear displacements of different material points at the other three flow lines (#2–#4), we use a method similar to [Giovanola 1988]. The three flow lines in high-speed photographs [Marchand and Duffy 1988; Cho et al. 1993; Liao and Duffy 1998] in the present work are marked in Figure 3. In Figure 3(a), taken from [Liao and Duffy 1998], in Figure 3(b), taken from [Cho et al. 1993], and in Figure 3(c), taken from [Marchand and Duffy 1988], there exist many flow lines. In the present work, only the results for a typical flow line in each figure are presented since selecting different flow lines from a figure results in the basically same results. For different frames in the same figure, data points on the same flow line are considered.

For the sake of simplicity, only a portion of the material points with the same horizontal spacing at each flow line is selected. Let the number of the selected material points be N_0. The leftmost material point is the first point. During the dynamic torsion, a short thin-walled tubular specimen is sandwiched between two long elastic bars, called the input bar and output bar. Near the loading ends, the stress and strain within the specimen is quite complex, possibly deviating from the simple pure shear state. Therefore, the data from material points near the two ends must be omitted in fitting. The remaining data will be fitted, and the total number of fitted data points is $N = N_0 - N_0^l - N_0^r$, where N_0^l and N_0^r are the numbers of omitted data points near the left and right ends of the specimen, respectively. Those data points, deviating from the slopes of the grid lines of the uniformly deformational regions outside the ASB, are omitted. Thus, the values of N_0^l and N_0^r can be determined easily.

These fitted data can be divided into three groups. The number of data points in the groups is denoted by N_1, N_2, and N_3, respectively. The first group is from the (N_0^l+1)-th to the $(N_0^l+N_1)$-th data point; the second from the $(N_0^l+N_1)$-th to the $(N_0^l+N_1+N_2-1)$-th; and the third from the $(N_0^l+N_1+N_2-1)$-th to the $(N_0^l+N_1+N_2+N_3-2)$-th. For the first and third groups, the line-fitting least-squares method is used, while for the second the curve-fitting least-squares method is used.

The extracted position and corresponding relative shear displacement of a material point is expressed as (y_i, d_i), $i = N_0^l + 1, N_0^l + 2, \ldots, N_0^l + N$. For the first group data, no special requirement on the theoretical expression (14) is enforced in fitting:

$$s(y, c_{11}, c_{12}) = c_{11} + c_{12}y. \tag{17}$$

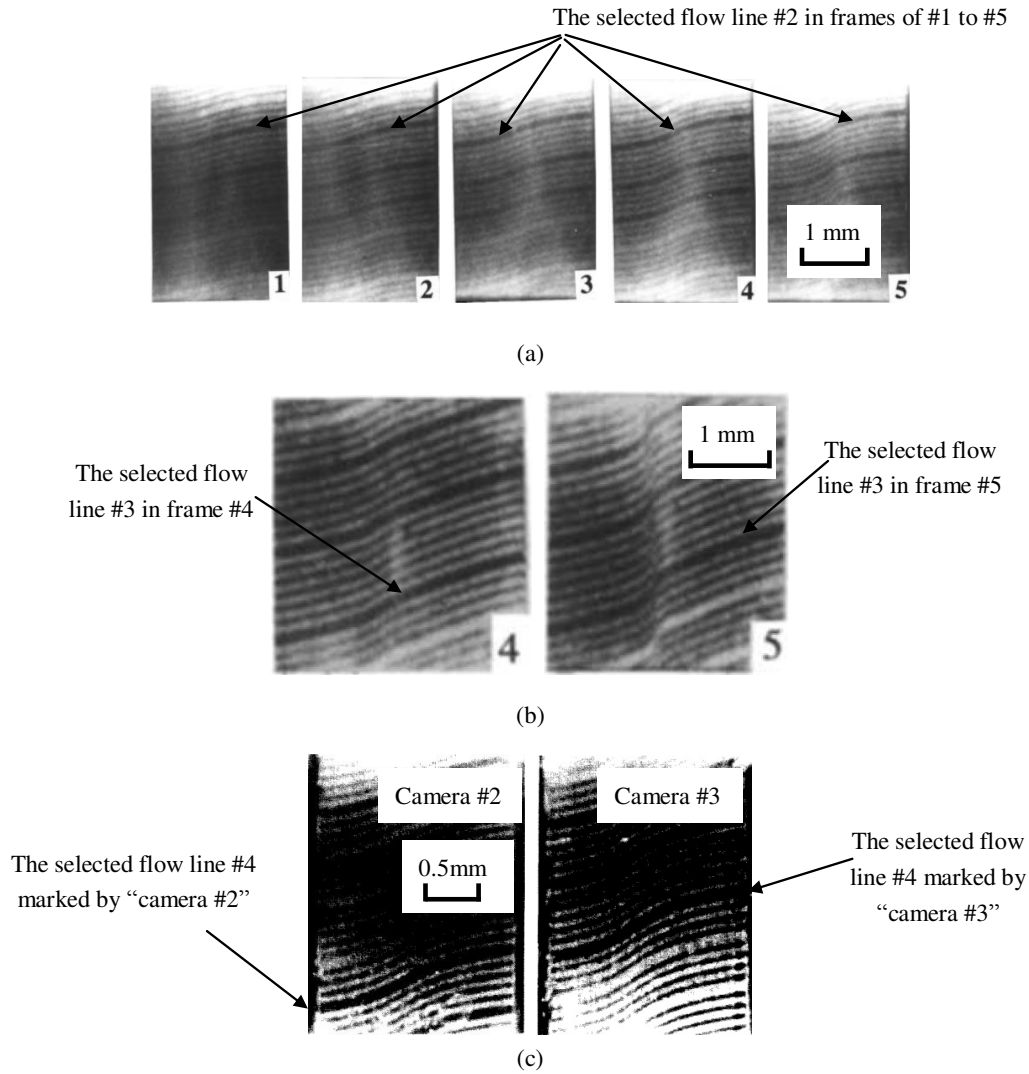

Figure 3. Selected flow lines from which coordinates and corresponding shear displacements are extracted: (a) the evolution of flow line #2 with straining for Ti-6Al-4V [Liao and Duffy 1998], (b) the evolution of flow line #3 with straining for HY-100 steel [Cho et al. 1993], and (c) flow line #4 in photographs taken at different positions using different cameras for HY-100 steel [Marchand and Duffy 1988].

For the second group data, it is required that the point $(y_{N_0^l+N_1}, d_{N_0^l+N_1})$ is at the theoretical curve, that is, (15), when $y = L^l$:

$$s(y, c_{21}, c_{22}) = d_{N_0^l+N_1} + c_{21}(y - L^l) + c_{22} \sin \frac{y - w/2 - L^l}{l}. \tag{18}$$

Similarly to the first group data, no special requirement is imposed on the theoretical expression, that

is, (16), for the third group data in fitting:

$$s(y, c_{31}, c_{32}) = c_{31} + c_{32}(y - L^l - w). \tag{19}$$

For the known N_1, N_2, and N_3 (or N_1, N_2, and N), using the fitting least-squares method results in values of c_{11}, c_{12}, c_{21}, c_{22}, c_{31}, and c_{32}. These values minimize the sum of the squared errors ($R_1^2 + R_2^2 + R_3^2$, R_1^2, R_2^2, and R_3^2 are the squared errors in the three groups of fitted data):

$$J_0 = \min(R_1^2 + R_2^2 + R_3^2) = \min\Big\{ \sum_{i=N_0^l+1}^{N_0^l+N_1} [d_i - s(y_i, c_{11}, c_{12})]^2 + \sum_{i=N_0^l+N_1}^{N_0^l+N_1+N_2-1} [d_i - s(y_i, c_{21}, c_{22})]^2 + \sum_{i=N_0^l+N_1+N_2-1}^{N_0^l+N} [d_i - s(y_i, c_{31}, c_{32})]^2 \Big\}. \tag{20}$$

For the given N, and different N_1 and N_2, the value of J_0 will be different. It is assumed that the true values of c_{11}, c_{12}, c_{21}, c_{22}, c_{31}, and c_{32} minimize J_0:

$$J = \min J_0. \tag{21}$$

During the search process, the ranges of N_1 and N_2 need to be specified. Thus, J_0 will be a spatially curved surface whose height is dependent on the values of N_1 and N_2. Finding a global minimum J_0 is easy. After that, the corresponding values of N_1 and N_2 are known. Thus c_{11}, c_{12}, c_{21}, c_{22}, c_{31}, and c_{32} will be specific, and the ASB width will also be obtained, which is only dependent on the data number N_2 in the second group, and the horizontal distance Δh of two adjacent data points. The ASB width w is then expressed as

$$w = (N_2 - 1)\Delta h. \tag{22}$$

Using (5), the internal length parameter will be obtained:

$$l = (N_2 - 1)\Delta h/2\pi. \tag{23}$$

Table 2 shows the selected parameters (N, N_0, N_0^l, N_0^r, and Δh) and obtained results (N_1, N_2, c_{12}, c_{21}, c_{22}, c_{32}, and w) corresponding to the minimum J_0. It is found that c_{21} and c_{22} have an increasing tendency with time (for flow line #1) and frame number (for flow lines of #2 and #3). The values of c_{11} (small enough) and c_{31} are not presented in Table 2 since the two parameters are independent of strain, that is, the slope of the local shear displacement. During the shear localization, the ASB width is found to become narrow or thin. Using the gradient plasticity theory with a variable length scale parameter, Voyiadjis and Abu Al-Rub [2005] argued that the length scale parameter should not be seen as a constant, and decreases with an increase of the plastic deformation. This finding is in agreement with the present work. Physically, the occurrence of highly elongated and fine grains, parallel to the shear direction due to the severe plastic shear deformation, is responsible for this phenomenon. Figures 4–7 show comparisons between the measured results and the best theoretical results with the obtained parameters after fitting listed in Table 2. Displacements of material points are relative to the first material point (the leftmost material point among the selected material points). The omitted material points outside the uniformly deformational regions and corresponding shear displacements are not depicted in Figures 4–7. The best

	Flow line #1			
Loading time =	45 μs	47.5 μs	50 μs	52.5 μs
N_0	76	76	76	76
N	43	43	43	43
N_0^l	17	17	17	17
N_0^r	17	17	17	17
$\Delta h/10^{-5}$ m	2.0	2.0	2.0	2.0
$J/10^{-10}$ m^2	0.1	0.2	1.2	7.6
N_1	17	17	17	19
N_2	10	9	9	4
c_{12}	0.127	0.130	0.138	0.147
c_{21}	0.241	0.457	0.830	2.565
$c_{22}/10^{-6}$ m	0.33	8.35	21.12	32.21
c_{32}	0.175	0.180	0.192	0.237
$w/10^{-4}$ m	2.0	1.8	1.8	0.8

	Flow line #2					Flow line #3		Flow line #4	
	Frame #1	Fr. #2	Fr. #3	Fr. #4	Fr. #5	Fr. #4	Fr. #5	Camera #2	Cam. #3
N_0	41	41	41	41	41	46	43	43	43
N	36	36	36	36	36	45	42	42	42
N_0^l	4	4	4	4	4	1	1	1	1
N_0^r	2	2	2	2	2	1	1	1	1
$\Delta h/10^{-5}$ m	4.9	4.9	4.9	4.9	4.9	6.2	6.7	4.3	4.3
$J/10^{-10}$ m^2	1.4	3.0	2.7	4.8	6.7	15.3	24.1	7.0	5.0
N_1	6	8	6	9	4	14	14	9	8
N_2	21	21	20	18	23	12	9	21	20
c_{12}	0.167	0.167	0.157	0.190	0.167	0.274	0.274	0.211	0.191
c_{21}	0.278	0.297	0.332	0.410	0.418	0.495	0.858	0.409	0.509
$c_{22}/10^{-6}$ m	5.59	4.60	8.37	8.01	33.05	12.67	57.28	22.23	19.18
c_{32}	0.162	0.160	0.183	0.167	0.177	0.334	0.385	0.204	0.208
$w/10^{-4}$ m	10	10	9.8	8.8	11	7.5	6.0	9.1	8.6

Table 2. Parameters used in fitting least-squares methods and fitted results for four flow lines.

theoretical results correspond to the minimum J_0. It is found that the agreement between the two kinds of results is good. This means that the second-order plastic strain gradient plays an important role in the postlocalization deformational stage of metal materials. The displacement distribution of a flow line in the deformed ASB can be described accurately by the linear and sinusoidal terms with respect to the material point coordinate beside a constant term.

It is also found that shear strains (c_{12} and c_{32}) in uniformly deformational bodies outside the ASB are slightly different. The wall thickness of the specimen, showing small variations along the length of the specimen [Liao and Duffy 1998], can be the reason for this phenomenon.

The calculated ASB width is usually larger than reported results [Giovanola 1988; Marchand and Duffy 1988; Cho et al. 1993; Liao and Duffy 1998]. In fact, the calculated width is the width of the

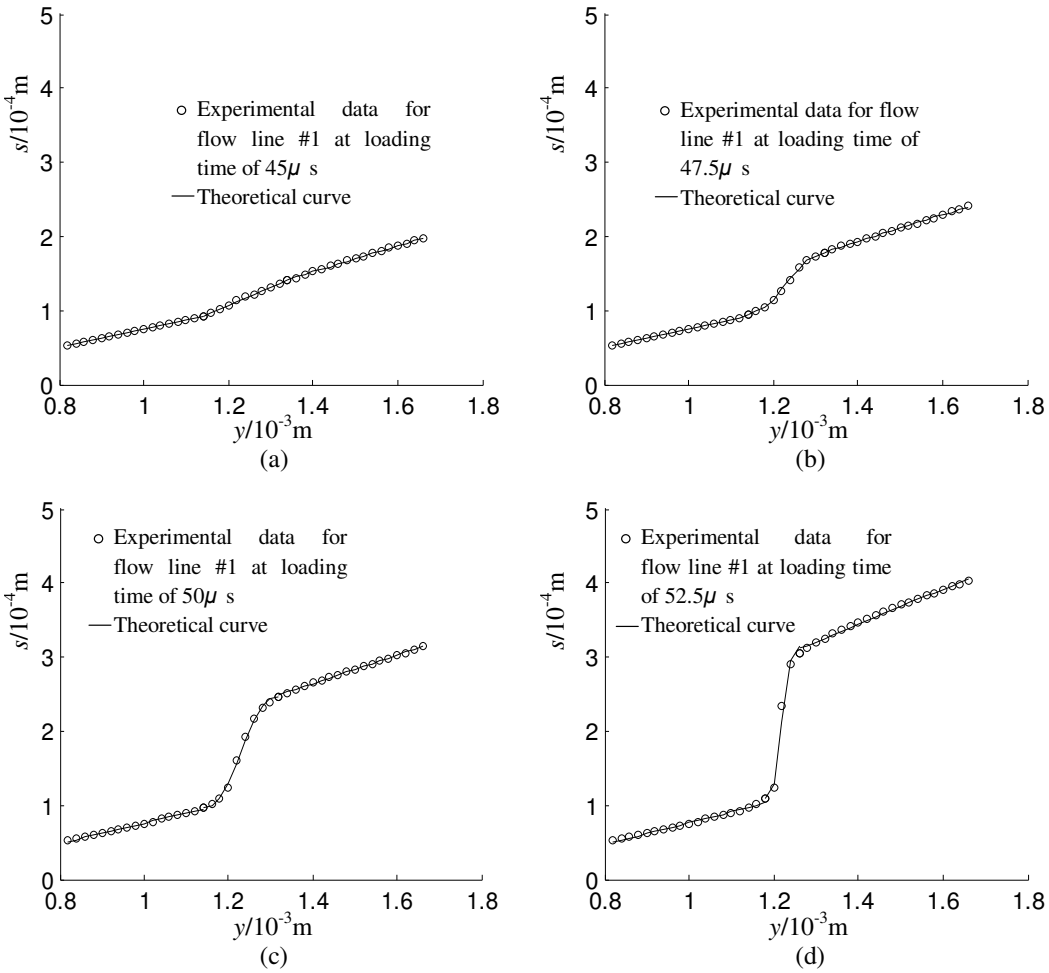

Figure 4. Comparisons of the measured shear displacements of material points at flow line #1 with loading time for 4340 steel [Giovanola 1988], and the fitted theoretical results based on second-order GDP with best parameters.

region with nonuniform strains, that is, the width of the deformed ASB. However, the reported width is usually the width of the ASB at its central region, over which the shear strain remains constant [Giovanola 1988; Marchand and Duffy 1988; Cho et al. 1993; Liao and Duffy 1998].

As mentioned before, theoretically, the critical plastic shear strain γ_c may be a constant for a flow line during the localized shear process. When the plastic shear strain within the specimen reaches γ_c, shear localization is assumed to occur. From (15) and (18), we can obtain the following expression:

$$c_{21} = \bar{\gamma}_p + \gamma^e, \quad c_{22} = l(\bar{\gamma}_p - \gamma_c), \tag{24}$$

$$\gamma_c = c_{21} - \frac{c_{22}}{l} - \gamma^e. \tag{25}$$

If the static shear Hooke's law ($\gamma^e = \tau/G$, where G is the shear elastic modulus that is the slope of the measured shear stress-nominal shear strain curve prior to the yield plateau) is used, then it is found that

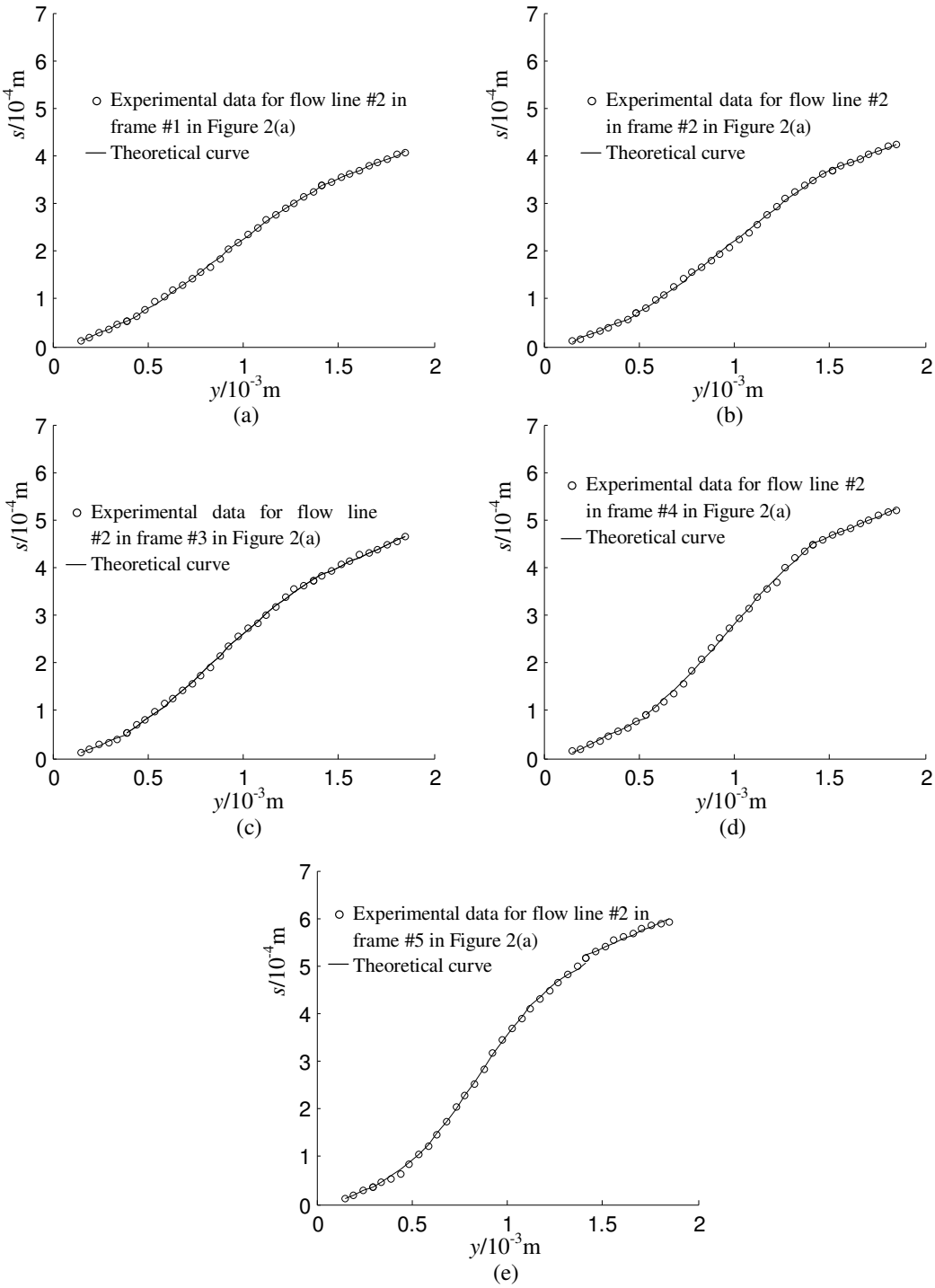

Figure 5. Comparisons of the measured shear displacements of material points at flow line #2 with straining for Ti-6Al-4V [Liao and Duffy 1998], and the fitted theoretical results based on second-order GDP with best parameters.

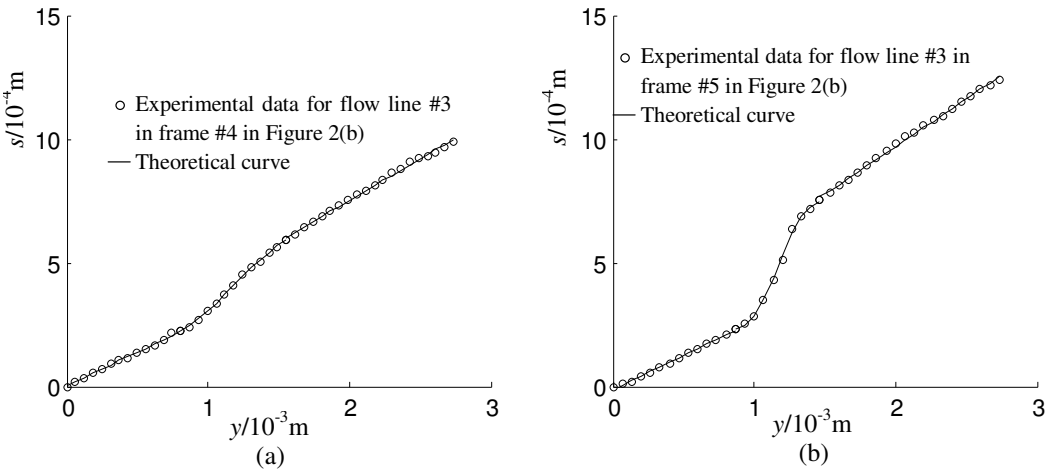

Figure 6. Comparisons of the measured shear displacements of material points at flow line #3 with straining for HY-100 steel [Cho et al. 1993], and the fitted theoretical results based on second-order GDP with best parameters.

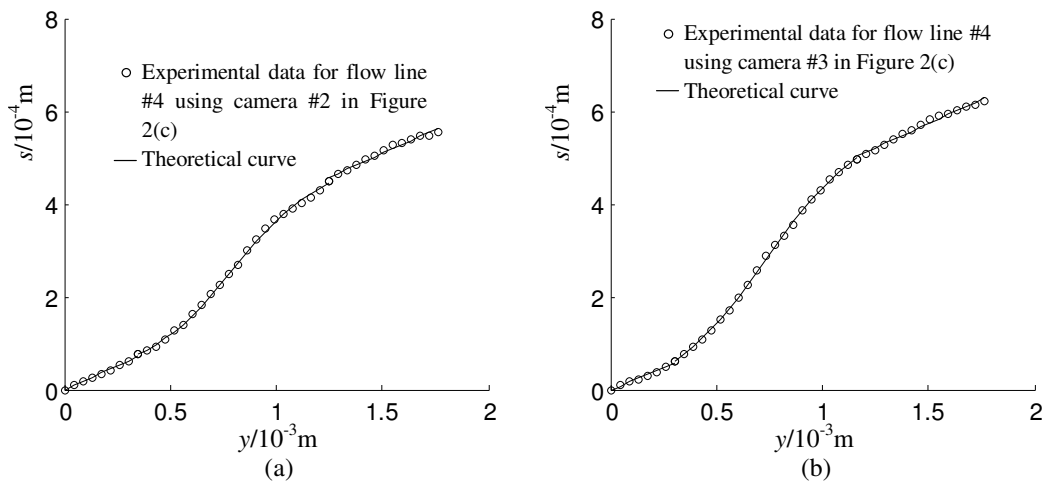

Figure 7. Comparisons of the measured shear displacements of material points at flow line #4 for HY-100 steel at the same time using different cameras [Marchand and Duffy 1988], and the fitted theoretical results based on second-order GDP with best parameters.

the calculated values of γ_c are variant using the obtained values of parameters (c_{21}, c_{22}, N_2, and Δh), the measured shear stress τ, and the shear elastic modulus G. The reason for this is still unclear. Seemingly, the static shear Hooke's law should not be used. An inertial effect must exist in dynamic torsional tests, possibly leading to a nonuniform shear stress distribution within the specimen to some extent. On the other hand, local perturbation (such as a microstructural inhomogeneity or machining marks) [Giovanola 1988] also possibly results in the nonuniform shear stress, even before shear localization. Even shear localization is initiated at postpeak, not at the highest shear strain within the specimen [Giovanola 1988].

Geometric defects have a key influence on the ASB initiation [Liao and Duffy 1998]. These factors are difficult to take into account in analyses. Obtaining a constant γ_c will require further investigation.

Damage during the shear yield process and beyond, and local rapid temperature rise in the ASB and the following heat conduct, possibly increase the plastic shear strain and displacement of material points. Thus, the expressions for c_{21} and c_{22} can be different from those in (24). The present expression is limited to the conditions without the damage and heat conduct. An analytical expression considering these factors is quite necessary.

4. Conclusions

During shear localization, the thin-walled tubular specimen within the gage length in dynamic torsion is simplified into three parts: two uniformly deformational regions surrounding the adiabatic shear band (ASB) and a central localized deformational region. Deformations in these regions are treated as one-dimensional shear problems. A linear distribution is assumed for the shear displacements of material points outside the ASB at a flow line. For arbitrary strain-softening materials in which certain plastic shear strains have accumulated before the ASB initiation, an expression for the shear displacement distribution in the ASB is established based on second-order gradient-dependent plasticity (GDP) considering the microstructural effect, including the linear and nonlinear (sinusoidal) terms with respect to the material point coordinate as well as a constant term.

To obtain the coefficients of the constant, linear, and nonlinear terms, which are not easy to determine due to the influence of geometric defects, line and curve-fitting least-squares methods are used for data in the uniform and localized deformational regions, respectively. For three kinds of materials, results show that the agreement between the measured shear displacements of flow lines using high-speed photography and the theoretical results is good. Moreover, the coefficients of the linear and sinusoidal terms with respect to the material point coordinate basically increase with loading time or straining during the shear localization process, while the ASB width has a decreasing tendency. The agreement suggests that second-order GDP is suitable for measuring the relative shear displacement distribution of flow lines in the ASBs.

If various parameters are known, flow lines can be numerically calculated by use of finite-element methods where enriched continuum models are necessarily included, avoiding pathological mesh sensitivity. However, these parameters are possibly difficult to specify. Using the proposed analytical expression for the local shear displacement in the ASB and outside, under the condition of unknown parameters, these parameters, such as the width of the ASB, and the critical plastic shear strain corresponding to the onset of the localized deformation, can be determined together by fitting with experimental observations. The fitted width of the ASB is apparently higher than the experimentally reported value. If the parameters obtained through fitting are used in the gradient-enhanced finite-element methods, then more accurate numerical results can be expected.

Acknowledgement

We are grateful to two anonymous reviewers for their helpful comments and suggestions in improving the manuscript. This work was supported by the Doctor Startup Foundation of Liaoning Province, China, No. 20081102, and supported by the Program for Liaoning Excellent Talents in University (LJQ2011030).

References

[Askes et al. 2000] H. Askes, J. Pamin, and R. De Borst, "Dispersion analysis and element-free Galerkin solutions of second- and fourth-order gradient-enhanced damage models", *Int. J. Numer. Methods Eng.* **49** (2000), 811–832.

[Bai and Bodd 1992] Y. Bai and B. Bodd, *Adiabatic shear localization: occurrence, theories and applications*, Pergamon Press, Oxford, 1992.

[Bažant and Pijaudier-Cabot 1988] Z. P. Bažant and G. Pijaudier-Cabot, "Nonlocal continuum damage, localization instability and convergence", *J. Appl. Mech.* (*ASME*) **55** (1988), 287–293.

[Cho et al. 1993] K. M. Cho, S. Lee, S. R. Nutt, and J. Duffy, "Adiabatic shear band formation during dynamic torsional deformation of an HY-100 steel", *Acta Metall. Mater.* **41** (1993), 923–932.

[De Borst and Mühlhaus 1992] R. De Borst and H. B. Mühlhaus, "Gradient-dependent plasticity: formulation and algorithmic aspects", *Int. J. Numer. Methods Eng.* **35** (1992), 521–539.

[Duffy and Chi 1992] J. Duffy and Y. C. Chi, "On the measurement of local strain and temperature during the formation of adiabatic shear bands", *Mater. Sci. Eng. A* **157** (1992), 195–210.

[Giovanola 1988] J. H. Giovanola, "Adiabatic shear banding under pure shear loading, I: Direct observation of strain localization and energy dissipation measurements", *Mech. Mater.* **7** (1988), 59–72.

[Liao and Duffy 1998] S. C. Liao and J. Duffy, "Adiabatic shear bands in a Ti-6Al-4V titanium alloy", *J. Mech. Phys. Solids* **46** (1998), 2201–2231.

[Marchand and Duffy 1988] A. Marchand and J. Duffy, "An experimental study of the formation process of adiabatic shear bands in a structural steel", *J. Mech. Phys. Solids* **36** (1988), 251–283.

[Menzel and Steinmann 2000] A. Menzel and P. Steinmann, "On the continuum formulation of higher gradient plasticity for single and polycrystals", *J. Mech. Phys. Solids* **48**:8 (2000), 1777–1796.

[Pamin and De Borst 1995] J. Pamin and R. De Borst, "A gradient plasticity approach to finite element predictions of soil instability", *Arch. Mech.* **47**:2 (1995), 353–377.

[Peerlings 2007] R. H. J. Peerlings, "On the role of moving elastic-plastic boundaries in strain gradient plasticity", *Model. Simul. Mater. Sci. Eng.* **15**:1 (2007), s109–s120.

[Peerlings et al. 2001] R. H. J. Peerlings, M. G. D. Geers, R. De Borst, and W. A. M. Brekelmans, "A critical comparison of nonlocal and gradient-enhanced softening continua", *Int. J. Solids Struct.* **38** (2001), 7723–7746.

[Poh et al. 2011] L. H. Poh, R. H. J. Peerlings, M. G. D. Geers, and S. Swaddiwudhipong, "An implicit tensorial gradient plasticity model-formulation and comparison with a scalar gradient model", *Int. J. Solids Struct.* **48** (2011), 2595–2604.

[Rittel et al. 2006] D. Rittel, Z. G. Wang, and M. Merzer, "Adiabatic shear failure and dynamic stored energy of cold work", *Phys. Rev. Lett.* **96**:7 (2006), Article ID #075502.

[Shawki and Clifton 1989] T. G. Shawki and R. J. Clifton, "Shear band formation in thermal visco-plastic materials", *Mech. Mater.* **8** (1989), 13–43.

[Simone et al. 2004] A. Simone, H. Askes, R. H. J. Peerlings, and L. J. Sluys, "Interpolation requirements for implicit gradient-enhanced continuum damage models", *Commun. Numer. Methods Eng.* **20** (2004), 163–165.

[Voyiadjis and Abu Al-Rub 2005] G. Z. Voyiadjis and R. K. Abu Al-Rub, "Gradient plasticity theory with a variable length scale parameter", *Int. J. Solids Struct.* **42** (2005), 3998–4029.

[Wang 2006a] X. B. Wang, "Temperature-dependent shear strain localization of aluminum-lithium alloy in uniaxial compression using Zerilli–Armstrong and gradient plasticity models", *Mater. Sci. Forum* **519-521** (2006), 789–794.

[Wang 2006b] X. B. Wang, "Temperature distribution in adiabatic shear band for ductile metal based on Johnson–Cook and gradient plasticity models", *Trans. Nonferr. Met. Soc. China* **16** (2006), 333–338.

[Wang 2006c] X. B. Wang, "Effects of constitutive parameters on adiabatic shear localization for ductile metal based on Johnson–Cook and gradient plasticity models", *Trans. Nonferr. Met. Soc. China* **16** (2006), 1362–1369.

[Wang 2007] X. B. Wang, "Adiabatic shear localization for steels based on Johnson–Cook model and second- and fourth-order gradient plasticity models", *J. Iron Steel Res. Int.* **14** (2007), 56–61.

[Wang 2008] X. B. Wang, "Effects of temperature and strain rate on the evolution of thickness of transformed adiabatic shear band", *Solid State Phenom.* **138** (2008), 385–392.

[Wang 2009] X. B. Wang, "Theoretical analysis of the adiabatic shear band width and strain rate effect of Ti-6Al-4V", *Rare Met. Mater. Eng.* **38** (2009), 214–218. In Chinese.

[Wang 2010] X. B. Wang, "A new method for calculating the peak temperature evolution in the adiabatic shear band of steel", *J. Mech. Mater. Struct.* **5** (2010), 95–106.

Received 27 Oct 2011. Revised 28 Jun 2012. Accepted 27 Jul 2012.

XUE-BIN WANG: wxbbb@263.net
Department of Mechanical Science and Engineering, Liaoning Technical University, Fuxin City, 123000, China

BING MA: bingandna@263.net
Department of Mechanical Science and Engineering, Liaoning Technical University, Fuxin City, 123000, China

JOURNAL OF MECHANICS OF MATERIALS AND STRUCTURES

jomms.net

Founded by Charles R. Steele and Marie-Louise Steele

See http://jomms.net for submission guidelines.

JoMMS (ISSN 1559-3959) is published in 10 issues a year. The subscription price for 2012 is US $555/year for the electronic version, and $735/year (+$60 shipping outside the US) for print and electronic. Subscriptions, requests for back issues, and changes of address should be sent to Mathematical Sciences Publishers, Department of Mathematics, University of California, Berkeley, CA 94720–3840.

JoMMS peer-review and production is managed by EditFLOW® from Mathematical Sciences Publishers.

PUBLISHED BY

mathematical sciences publishers

http://msp.org/

A NON-PROFIT CORPORATION

Typeset in LaTeX

Journal of Mechanics of Materials and Structures

Volume 7, No. 8-9 October 2012